magnetic resonance imaging bolus tracking: comparison with positron emission tomography values. *J Cereb Blood Flow Metab* 18:425–32

Ostergaard L, Sorensen AG, Kwong KK, Weisskoff RM, Gyldensted C, Rosen BR (1996*a*) High resolution measurement of cerebral blood flow using intravascular tracer bolus passages. Part II: Experimental comparison and preliminary results. *Magn Reson Med* 36:726–36

Ostergaard L, Weisskoff RM, Chesler DA, Gyldensted C, Rosen BR (1996*b*) High resolution measurement of cerebral blood flow using intravascular tracer bolus passages. Part I: Mathematical approach and statistical analysis. *Magn Reson Med* 36:715–25

Powers WJ (1991) Cerebral hemodynamics in ischemic cerebrovascular disease. *Ann Neurol* 29:231–40

Powers WJ, Press GA, Grubb RL, Jr, Gado M, Raichle ME (1987) The effect of hemodynamically significant carotid artery disease on the hemodynamic status of the cerebral circulation. *Ann Intern Med* 106:27–34

Schreiber WG, Guckel F, Strizke P, Schmiedek P, Schwartz A, Brix G (1998) Cerebral blood flow and cerebrovascular reserve capacity: estimation by dynamic magnetic resonance imaging. *J Cereb Blood Flow Metab* 18: 1143–56

Senda M, Buxton RB, Alpert NM, Correia JA, Mackay BC, Weise SB, Ackerman RH (1988) The 15O steady-state method: correction for variation in arterial concentration. *J Cereb Blood Flow Metab* 8:681–90

Shimada Y, Uemura K, Ardekani BA, Nagaoka T, Ishiwata K, Toyama H, Ono K, Senda M (2000) Application of PET-MRI registration techniques to cat brain imaging. *J Neurosci Methods* 101:1–7

Suzuki J, Takaku A (1969) Cerebrovascular 'moyamoya' disease. Disease showing abnormal net-like vessels in base of brain. *Arch Neurol* 20:288–99

Tsuchiya K, Inaoka S, Mizutani Y, Hachiya J (1998) Echo-planar perfusion MR of moyamoya disease. *Am J Neuroradiol* 19:211–6

Warach S, Dashe JF, Edelman RR (1996) Clinical outcome in ischemic stroke predicted by early diffusion-weighted and perfusion magnetic resonance imaging: a preliminary analysis. *J Cereb Blood Flow Metab* 16: 53–9

Wu O, Ostergaard L, Koroshetz WJ, Schwamm LH, O'Donnell J, Schaefer PW, Rosen BR, Weisskoff RM, Sorensen AG (2003) Effects of tracer arrival time on flow estimates in MR perfusion-weighted imaging. *Magn Reson Med* 50:856–64

Yamada I, Himeno Y, Nagaoka T, Akimoto H, Matsushima Y, Kuroiwa T, Shibuya H (1999) Moyamoya disease: evaluation with diffusion-weighted and perfusion echo-planar MR imaging. *Radiology* 212:340–7

ELSEVIER

Journal of the Neurological Sciences 252 (2007) 88–91

Journal of the Neurological Sciences

www.elsevier.com/locate/jns

Short communication

A novel compound heterozygous mutation in the *DAP12* gene in a patient with Nasu-Hakola disease

Ryo Kuroda [a,*], Junichi Satoh [b,c], Takashi Yamamura [b], Toshiharu Anezaki [d], Tatsuhiro Terada [a], Kinya Yamazaki [a], Tomokazu Obi [a], Kouichi Mizoguchi [a]

[a] *Department of Neurology, Shizuoka Institute of Epilepsy and Neurological Disorders, 886 Urushiyama, Aoi-ku, Shizuoka 420-8688, Japan*
[b] *Department of Immunology, National Institute of Neuroscience, NCNP, 4-1-1 Ogawahigashi, Kodaira, Tokyo 187-8502, Japan*
[c] *Department of Bioinformatics and Neuroinformatics, Meiji Pharmaceutical University, 2-522-1 Noshio, Kiyose, Tokyo 204-8588, Japan*
[d] *Department of Neurology, Numazu City Hospital, 550 Harunoki, Higashishiinoji, Numazu, Shizuoka 410-0302, Japan*

Received 24 March 2006; received in revised form 21 August 2006; accepted 22 September 2006
Available online 27 November 2006

Abstract

A 34-year-old woman showed clinical features characteristic of Nasu-Hakola disease (NHD), also designated polycystic lipomembranous osteodysplasia with sclerosing leukoencephalopathy (PLOSL). The genetic analysis of the *DAP12* gene (*TYROBP*) identified two heterozygous mutations composed of a previously reported single base deletion of 141G (141delG) in exon 3 and a novel single base substitution of G262T in exon 4, both of which are located on separate alleles. The protein sequence motif search indicated that both mutations encode truncated nonfunctional DAP12 polypeptides. This is the first case of NHD caused by compound heterozygosity for loss-of-function mutations in *DAP12*.

Keywords: Compound heterozygote; DAP12; Loss of function mutations; TYROBP; Nasu-Hakola disease

1. Introduction

Nasu-Hakola disease (NHD; OMIM 221770), also designated polycystic lipomembranous osteodysplasia with sclerosing leukoencephalopathy (PLOSL), is a rare autosomal recessive disorder characterized by a combination of progressive presenile dementia and formation of multifocal bone cysts filled with thickened adipocyte membranes [1]. The clinical course of NHD is divided into four stages: (i) the latent stage with normal early development, (ii) the osseous stage beginning at the third decade of life, characterized by pain and swelling in ankles and feet followed by frequent bone fractures, (iii) the early neuropsychiatric stage occurring at the fourth decade of life, presenting with a frontal lobe syndrome such as euphoria and loss of social inhibitions, and (iv) the late neuropsychiatric stage, characterized by profound dementia, loss of mobility, and death usually by age 50 years [2].

NHD is caused by a structural defect in one of the two genes, *DAP12* on chromosome 19q13.1, alternatively named TYRO protein tyrosine kinase-binding protein (*TYROBP*), and *TREM2* on chromosome 6p21.1 [2–5]. The *DAP12* gene encodes DNAX-activation protein 12 (DAP12), a transmembrane adaptor protein that associates with several cell surface receptors, including triggering receptor expressed on myeloid cells 2 (TREM2). Because DAP12 is widely expressed in lymphoid and myeloid lineage cells, including natural killer (NK) cells, monocytes/macrophages, dendritic cells (DC), osteoclasts, and brain microglia, DAP12 signaling regulates a broad range of immune responses, along with differentiation of osteoclasts [6]. At present, 16 different NHD-causing

* Corresponding author. Department of Neurology, Yaizu City Hospital, 1000 Dobara, Yaizu, Shizuoka 425-8505, Japan. Tel.: +81 54 623 3111; fax: +81 54 624 9103.
E-mail address: ryou.kuroda@hospital.yaizu.shizuoka.jp (R. Kuroda).

0022-510X/$ - see front matter © 2006 Elsevier B.V. All rights reserved.
doi:10.1016/j.jns.2006.09.019

Fig. 1. Biopsy specimen of bone cyst. Dystrophic bone tissues characterized by the presence of alveolar membranous structures (HE, magnification ×200).

mutations are identified in *DAP12* or *TREM2* [2]. They include a large deletion of exons 1 to 4 of *DAP12* identified in all Finnish patients and a population of Swedish and Norwegian patients [3], and one base deletion of 141G (141delG) in exon 3 of *DAP12* in several Japanese patients [4], and a single base substitution of G233A in exon 2 of *TREM2* in two Swedish families [5]. All affected individuals are homozygous for the disease-causing mutations.

In the present report, we describe the first case of NHD caused by compound heterozygosity for two different loss-of-function mutations, 141delG and G262T, in the *DAP12* gene.

2. Materials and methods

High molecular weight genomic DNA was extracted from 300 μl of whole peripheral blood samples using the GenomicPreP blood DNA isolation kit (Amersham Bioscience). All five exons and 5′ and 3′ flanking regions of the *DAP12* gene (*TYROBP*; GenBank accession No. AF019563) were amplified by PCR using the primer sets specific for individual exons [3]. The purified PCR products were processed for direct sequencing by the dideoxynucleotide chain termination method on ABI PRIZM 3100 Genetic Analyzer (Applied Biosystems). To verify the heterozygosity of the mutations, genomic DNA amplified by PCR using exon 3 sense and exon 4 antisense primers were cloned into pcDNA4/HisMax-TOPO vector (Invitrogen), followed by processing for sequencing analysis. Specific protein sequence motifs were surveyed by the database search on the Scansite Motif Scanner under the high stringent condition [7].

3. Case report and results of genetic analysis

3.1. Case report

A 34-year-old woman was admitted to the hospital because of progressive mental disturbance. She has no family history of recurrent bone fractures. Her parents were not consanguineous. Her parents are in good health over age 70, while her paternal grandmother died of dementia at age 80. Until age 30, she experienced bone fractures of distal extremities 3 times following trivial accidents. At age 30, her husband noticed her memory disturbance and personality change characterized by emotional lability and irritability. At age 32, an X-ray examination showed multicystic lesions distributed bilaterally in distal ends of tibia and fibula. The bone biopsy specimen was compatible with lipomembranous osteodysplasia (Fig. 1).

On neurological examination, she was almost normal except for mild spastic gait and hyperactive deep-tendon reflexes in both upper and lower extremities. The Wechsler Adult Intelligence Scale-revisited (WAIS-R) score was 76 in total intelligence quotient (IQ). The Rivermead Behavioural Memory test (RBMT) suggested the presence of mild cognitive impairment. Brain MRI showed high intensity lesions in the bilateral periventricular white matter and internal capsule on T2-weighted and fluid-attenuated inversion recovery (FLAIR) images (Fig. 2a), while low intensity lesions indicative of ferritin storage were found in the bilateral basal ganglia and thalamus on T2-weighted and FLAIR images (Fig. 2b). An electroencephalogram (EEG) and somatosensory evoked potential (SEP) were interpreted as normal. The routine laboratory examination of blood was normal. The plasma very long chain fatty acid (VLFA) C26:0/C22:0 ratio (0.005) was normal. All of neurological and radiological observations described above supported a clinical diagnosis of NHD.

3.2. Identification of a novel heterozygous mutation in the DAP12 gene

After written informed consent was obtained, peripheral blood was processed for genetic analysis. PCR and direct sequencing analysis of five exons and exon-intron boundaries of the *DAP12* gene identified two different mutations composed of a single base deletion of 141G (141delG) in exon 3 (Fig. 3a) and a single base substitution of G262T in exon 4

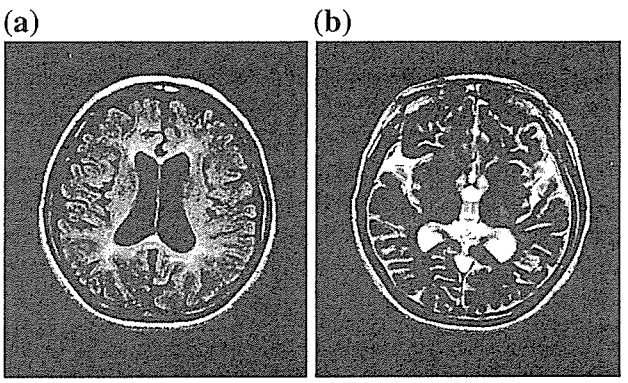

Fig. 2. Brain MRI. (a) High intensity lesions in the bilateral periventricular white matter on an axial FLAIR image (TR: 8000 ms, TE: 120 ms). (b) Low intensity lesions in the bilateral basal ganglia on an axial T2-weighted image (TR: 4000 ms, TE: 102 ms).

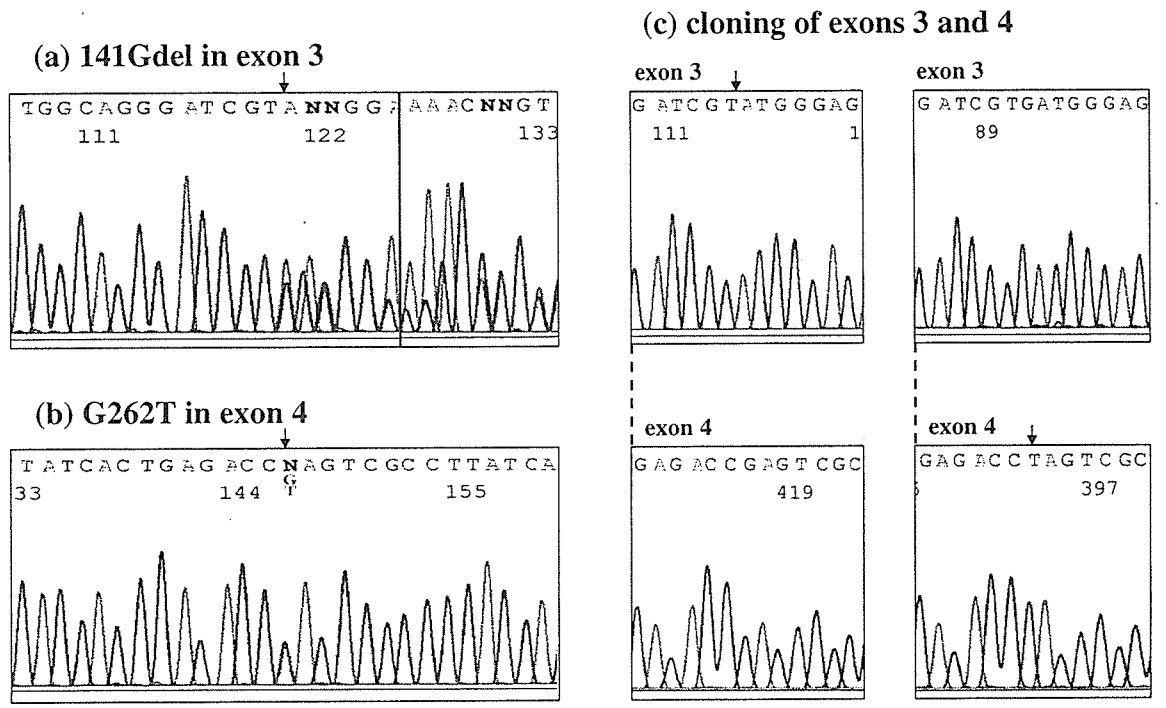

Fig. 3. Sequencing analysis of the *DAP12* gene. All five exons and exon–intron boundaries of the *DAP12* gene were amplified from genomic DNA by PCR. PCR products were processed for direct sequencing analysis (a, b) or were cloned in a vector, followed by processing for sequencing analysis (c). The panels represent (a) a single base deletion of 141G (141delG) in exon 3, (b) a single base substitution of G262T in exon 4, and (c) the heterozygosity of 141delG and G262T mutations verified by cloning of the segment spanning exons 3 and 4.

(Fig. 3b). The former caused a frameshift in the open reading frame (ORF), thereby causing premature termination of the polypeptide chain at amino acid residue 52 (Fig. 4c) [3,4]. The latter is a novel mutation which replaced glutamic acid (GAG) by a termination codon (TAG), resulting in premature termination of the polypeptide chain at amino acid residue 87 (Fig. 4b). The heterozygosity of two distinct mutations was verified by cloning and sequencing of PCR products of the segment spanning exons 3 and 4 (Fig. 3c). Protein sequence motif search on the Scansite Motif Scanner [7] showed that the G262T allele encodes a truncated DAP12 protein which contains a DAP10 membrane domain but no intracellular tyrosine-based activation motif (ITAM), while the 141delG allele codes for a shorter polypeptide that has no structural domains (Fig. 4a–c). These results indicate that the patient is a compound heterozygote having two distinct mutations in separate alleles of the *DAP12* ORF, both of which are nonfunctional.

4. Discussion

Here we reported a clinically typical NHD case caused by compound heterozygosity for two different mutations, 141delG and G262T, in the *DAP12* gene (*TYROBP*). Our previous study identified two mutations 141delG and T2C in Japanese NHD patients [4]. The G262T mutation we

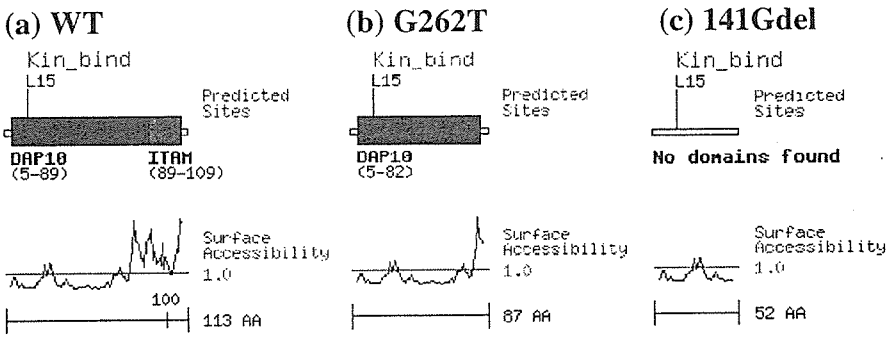

Fig. 4. Protein sequence motif analysis of two distinct DAP12 mutants. Protein sequence motifs were analyzed by the Scansite Motif Scanner. (a) the wild-type DAP12 protein, (b) the G262T mutant protein, and (c) the 141delG mutant protein. DAP10, ITAM, and "Kin_bind" represent a DAP10 membrane domain, an immunoreceptor tyrosine-based activation motif, and a consensus sequence for the mitogen-activated kinase (MAPK1) binding site, respectively. A plot of the surface accessibility shows residues that are likely to be near the protein surface and thus potentially bind to interacting proteins.

identified in the present study is the third one found in Japanese NHD patients.

Although various loss-of-function mutations were identified in NHD patients in the *DAP12* gene or the *TREM2* gene [2–5], the precise molecular and cellular mechanisms underlying the pathogenesis of NHD remain unknown. DAP12-deficient ($DAP12^{-/-}$) mice developed an increased bone mass (osteopetrosis), a reduction of myelin (hypomyelinosis) accentuated in the thalamus, and synaptic degeneration, suggesting that DAP12 signaling is essential for development of osteoclasts and oligodendrocytes and synaptogenesis [8]. NK cell and DC function is impaired in knock-in mice having a nonfunctional DAP12 ITAM motif (KΔY75) [9,10]. Differentiation of microglial cells is markedly inhibited and their function is altered in KΔY75 mice [11,12], suggesting a role of persistent microglial dysfunction in hypomyelination and aberrant synaptic plasticity in DAP12-deficient mice [13]. Importantly, differentiation of osteoclasts *in vitro* is delayed also in NHD patients, associated with a reduced bone resorption capability [14]. All of these observations suggest that the ITAM motif of DAP12, which is deleted in our patient with heterozygous mutations of 141delG and G262T, plays a pivotal role in signal transduction for development and differentiation of osteoclasts, oligodendrocytes, and microglia.

In addition to a great range of genetic heterogeneity, NHD clinically shows some phenotypic variability [1,2]. Bone fractures are diagnosed at the mean age of 27 years with a range of 18 to 33 years, while the mean age at onset of personality change is 33 years with a range of 25 to 40 years in NHD patients with homozygous mutations of the *DAP12* gene [1]. However, there exists no obvious difference in the clinical course between Japanese NHD patients homozygous for 141delG in *DAP12* [4] and a case of compound heterozygote we reported here, suggesting less importance of genetic variation but an involvement of as yet undefined nongenetic factors in development of phenotypic variability of NHD [2].

Acknowledgements

This work was in part supported by grants to J.-I.S and T.Y. from Research on Psychiatric and Neurological Diseases and Mental Health, the Ministry of Health, Labour and Welfare of Japan (H17-020), Research on Health Sciences Focusing on Drug Innovation, the Japan Health Sciences Foundation (KH21101), the Grant-in-Aid for Scientific Research, the Ministry of Education, Culture, Sports, Science and Technology (B18300118), and the Program for Promotion of Fundamental Studies in Health Sciences of the National Institute of Biomedical Innovation (NIBIO), Japan.

References

[1] Paloneva J, Autti T, Raininko R, Partanen J, Salonen O, Puranen M, et al. CNS manifestations of Nasu-Hakola disease. A frontal dementia with bone cysts. Neurology 2001;56:1552–8.
[2] Klünemann HH, Ridha BH, Magy L, Wherrett JR, Hemelsoet DM, Keen RW, et al. The genetic causes of basal ganglia calcification, dementia, and bone cysts. *DAP12* and *TREM2*. Neurology 2005;64:1502–7.
[3] Paloneva J, Kestilä M, Wu J, Salminen A, Böhling T, Ruotsalainen V, et al. Loss-of-function mutations in *TYROBP* (*DAP12*) result in a presenile dementia with bone cysts. Nat Genet 2000;25:357–61.
[4] Kondo T, Takahashi K, Kohara N, Takahashi Y, Hayashi S, Takahashi H, et al. Heterogeneity of presenile dementia with bone cysts (Nasu-Hakola disease). Three genetic forms. Neurology 2002;59:1105–7.
[5] Paloneva J, Manninen T, Christman G, Hovanes K, Mandelin J, Adolfsson R, et al. Mutations in two genes encoding different subunits of a receptor signaling complex result in an identical disease phenotype. Am J Hum Genet 2002;71:656–62.
[6] Tomasello E, Vivier E. KARAP/DAP12/TYROBP: three names and a multiplicity of biological functions. Eur J Immunol 2005;35:1670–7.
[7] Obenauer JC, Cantley LC, Yaffe MB. Scansite 2.0: Proteome-wide prediction of cell signaling interactions using short sequence motifs. Nucleic Acids Res 2003;31:3635–41.
[8] Kaifu T, Nakahara J, Inui M, Mishima K, Momiyama T, Kaji M, et al. Osteopetrosis and thalamic hypomyelinosis with synaptic degeneration in DAP12-deficient mice. J Clin Invest 2003;111:323–32.
[9] Tomasello E, Desmoulins P-O, Chemin K, Guia S, Cremer H, Ortaldo J, et al. Combined natural killer cell and dendritic cell functional deficiency in KARAP/DAP12 loss-of-function mutant mice. Immunity 2000;13:355–64.
[10] Sjölin H, Tomasello E, Mousavi-Jazi M, Bartolazzi A, Kärre K, Vivier E, et al. Pivotal role of KARAP/DAP12 adaptor molecule in the natural killer cell-mediated resistance to murine cytomegalovirus infection. J Exp Med 2002;195:825–34.
[11] Roumier A, Béchade C, Poncer J-C, Smalla K-H, Tomasello E, Vivier E, et al. Impaired synaptic function in the microglial KARAP/DAP12-deficient mouse. J Neurosci 2004;24:11421–8.
[12] Nataf S, Anginot A, Vuaillat C, Malaval L, Fodil N, Chereul E, et al. Brain and bone damage in KARAP/DAP12 loss-of-function mice correlate with alterations in microglia and osteoclast linages. Am J Pathol 2005;166:275–86.
[13] Takahashi K, Rochford CD, Neumann H. Clearance of apoptotic neurons without inflammation by microglial triggering receptor expressed on myeloid cells-2. J Exp Med 2005;201:647–57.
[14] Paloneva J, Mandelin J, Kiialainen A, Böhling T, Prudlo J, Hakola P, et al. DAP12/TREM2 deficiency results in impaired osteoclast differentiation and osteoporotic features. J Exp Med 2003;198:669–75.

Neuropathology 2006; **26**, 569–578 doi:10.1111/j.1440-1789.2006.00731.x

Case Report

Corticobasal degeneration as cause of progressive non-fluent aphasia: Clinical, radiological and pathological study of an autopsy case

Masaki Takao,[1,2] Kuniaki Tsuchiya,[3,4] Masaru Mimura,[5] Suketaka Momoshima,[6] Hiromi Kondo,[4] Haruhiko Akiyama,[4] Norihiro Suzuki,[2] Ban Mihara,[1] Yasuyuki Takagi[7] and Atsuo Koto[8]

Departments of [1]Neurology, Mihara Memorial Hospital, Isesaki, Gunma, [2]Neurology, School of Medicine, Keio University, Tokyo, [3]Laboratory Medicine and Pathology, Tokyo Metropolitan Matsuzawa Hospital, Tokyo, [4]Neuropathology, Tokyo Institute of Psychiatry, Tokyo, [5]Neuropsychiatry, Showa University School of Medicine, Tokyo, [6]Diagnostic Neuroradiology, School of Medicine, Keio University, Tokyo, [7]Neurology, Isuzu Hospital, Tokyo, and [8]Neurology, Yomiuriland Keiyu Hospital, Tokyo, Japan

A Japanese male developed gradual loss of spontaneous speech at age 60. Three years later meaningful speech had deteriorated to the point that it had become restricted to monotonous utterances. Neuropsychological examination at age 62 showed that he had severe non-fluent aphasia. A brain MRI demonstrated mild cortical atrophy with ischemic lesions in the cerebral white matter. He was diagnosed as having primary progressive aphasia. At age 63, he was admitted to the hospital to reevaluate the neurological condition. Neurologic examination showed severe non-fluent aphasia, hyperreflexia, snout and sucking reflexes. No alien hand was observed. He was able to walk, dress, wash himself and use chopsticks as well as name real objects. At age 65, ^{99m}Tc-hexamethylpropyleneamine oxime single photon emission computed tomography (HMPAO-SPECT) revealed diffuse cerebral hypoperfusion that was particularly prominent in the left frontal lobe. An MRI showed progressive cortical atrophy with the definite atrophy of the left paracentral gyrus. The hippocampal formation and putamen were also atrophic. He died of pneumonia at age 67. The brain weighed 810 g with atrophy of the frontal lobe, globus pallidus, enlargement of the lateral ventricles and depigmentation of the substantia nigra. Microscopic examination showed severe neuronal loss and gliosis in the cerebral cortex, globus pallidus interna and substantia nigra. Ballooned neurons were observed in the cerebral cortex. Gallyas-Braak method revealed numerous astrocytic plaques and argentophilic threads in the cerebrum. Clinical diagnosis of corticobasal degeneration sometimes is difficult in individuals with atypical clinical presentations. More exact clinical and radiological criteria may warrant a diagnosis of corticobasal degeneration.

Key words: argentophilic thread, astrocytic plaque, corticobasal degeneration, primary progressive aphasia, tauopathy.

INTRODUCTION

Corticobasal degeneration (CBD) or cortical-basal ganglionic degeneration was originally described by Rebeiz *et al.* as corticodentatonigral degeneration with neuronal achromasia.[1–3] CBD is a rare neurodegenerative disorder and clinically characterized by asymmetric limb clumsiness, rigidity, tremor, dystonia and cognitive dysfunction.[4–7] In an increased number of pathologically confirmed cases of CBD, clinical heterogeneity has been recognized. Based on the result of the recent large study, 93% of individuals with CBD showed various signs of higher cortical dysfunction, such as dyspraxia, cortical sensory loss, dementia and aphasia.[8] Aphasia has also been proposed as an important – but not universal – clinical symptom of CBD patients.[4] Thus, in those individuals, only limited cases have been pathologically confirmed as CBD. Furthermore, cognitive dysfunction as an initial presentation may still be an unusual manifestation of CBD.

Primary progressive aphasia is a clinical syndrome and is characterized by the gradual progression of impairment in word identification, object-naming, or word-comprehension without generalized dementia within the initial two years.[9–13] As an initial symptom of individuals

Correspondence: Masaki Takao, MD, Department of Neurology, Mihara Memorial Hospital, 366 Ohta, Isesaki 372-0006, Japan. Email: takao-jscn@umin.ac.jp

Received 1 February 2006; revised and accepted 22 March 2006.

with pathologically confirmed CBD, primary progressive aphasia is a relatively rare condition.[14–21]

In this paper, we report an autopsy case of CBD in which the patient developed progressive non-fluent aphasia as initial clinical presentation. This report will provide the information of clinical and neuropathologic heterogeneity as well as characteristic changes of MRI of CBD.

CASE REPORT

Clinical examination of the proband

The proband presented with neurological signs at 60 years of age. Throughout the eight-year long course of the disease, he underwent several neurological, neuropsychological and neuroradiological examinations.

Histology and immunohistochemistry

At autopsy, the brain of the proband was fixed in 10% formalin. Samples from the cerebral cortex, hippocampus, caudate nucleus, putamen, claustrum, globus pallidus, thalamus, amygdala, hypothalamus, subcortical nuclei, cerebellum, midbrain, pons and medulla were dehydrated in graded alcohol series, cleared in xylene and embedded in paraffin. Ten μm sections were stained with hematoxylin-eosin, the Holzer staining for gliosis, the Klüver-Barrera method for neuron and myelin, the Bodian silver staining for axons and modified Gallyas-Braak staining for abnormal tau protein.[3,22]

Immunohistochemical analysis of paraffin-embedded tissue blocks was carried out using an antigen retrieval method, to maximize the staining. Antibodies specific for neurofilament and glial fibrillary acidic protein (GFAP) were used.

Semi-quantitative analysis

Using modified Gallyas-Braak method, the frequency and distribution of Gallyas-Braak positive neurons (GBN) and astrocytic plaques (AP) were assessed semiquantitatively. A subjective scale was used to represent the numbers of GBN and AP (0 = none per 10× objective, 1 = up to 5 per 10× objective; 2 = 5–10 per 10× objective; 3 =10 per 10× objective). In addition, we evaluated argentophilic threads as well as the degree of neuronal loss and gliosis in each area.[23]

Clinical summary

The case of the individual reported here, a Japanese right-handed man, developed difficulties in speaking and in simple arithmetic calculation at age 60. He had been working as a baker since he was 28 years old and kept a small supermarket for the past 10 years. Since he felt a dull headache at age 60, a brain CT scan was carried out but showed no abnormal legions. He continued to exhibit gradual loss of spontaneous speech, although it was recorded that his memory seemed well preserved. A brain MRI showed an ischemic lesion of the right cerebral white matter adjacent to the posterior horn of the lateral ventricle. At age 61, his speech had further deteriorated. According to the medical chart, he showed difficulty in simple calculation, reading and writing. Memory disturbance was also recorded. He ceased working because he was unable to function well at the cash register. In the following two years his speech became restricted to monotonous utterances. The patient, approximately one year later, was referred to the neuropsychiatrist. Neuropsychologically, the condition of his speech was recognized as severe non-fluent aphasia. The patient could answer simple questions such as his name, age and his hometown. While he identified real objects such as a pencil and a pair of glasses, his spontaneous speech was non-fluent characterized with residual recurring utterances of "un" ("yes") or nodding. Perseveration, as well as simplification of speech and echolalia, was also present. Repetition was slightly impaired. Auditory comprehension appeared somewhat better than speech output, but was limited to simple commands such as "raise your hand". He failed even simple calculations (e.g., 1 + 2) both in oral and writing conditions. Indifference and lack of sympathy were noted as evidence of personality change. Mini-mental state examination scored 3/30, and he could not answer correctly even the first question of the Kohs block design test. A brain MRI demonstrated mild cortical atrophy with an ischemic lesion in the right parietal lobe. ^{123}I-IMP SPECT showed hypoperfusion in the bilateral frontal, temporal and parietal lobes. An electroencephalogram showed frequent slow waves with irregular and unsteady alpha waves. The individual was tentatively diagnosed as having primary progressive aphasia.

At age 63, he was admitted to the hospital to reevaluate his neurological condition. He still showed severe non-fluent aphasia. Although it was difficult to evaluate praxis and gnosia, no "alien hand" was observed. A neurologic examination revealed hyperreflexia in the all extremities, snout and sucking reflexes as well as disorientation. No dysphagia was observed. He was still able to walk, do dressing, use chopsticks and bathe. He could still name real objects such as a pencil, scissors, wallet, ruler and newspaper. Brain MRI demonstrated mild to moderate non-specific cerebral cortical atrophy without significant laterality. The hippocampal formation as well as basal ganglia appeared to be normal in size. Periventricular hyperintensity of moderate degree suggestive of diffuse ischemia was present. (Fig. 1A–D). Based on the medical record of the outpatient clinic at age 63, pathologic reflexes and rigidity were recorded. L-DOPA had never been adminis-

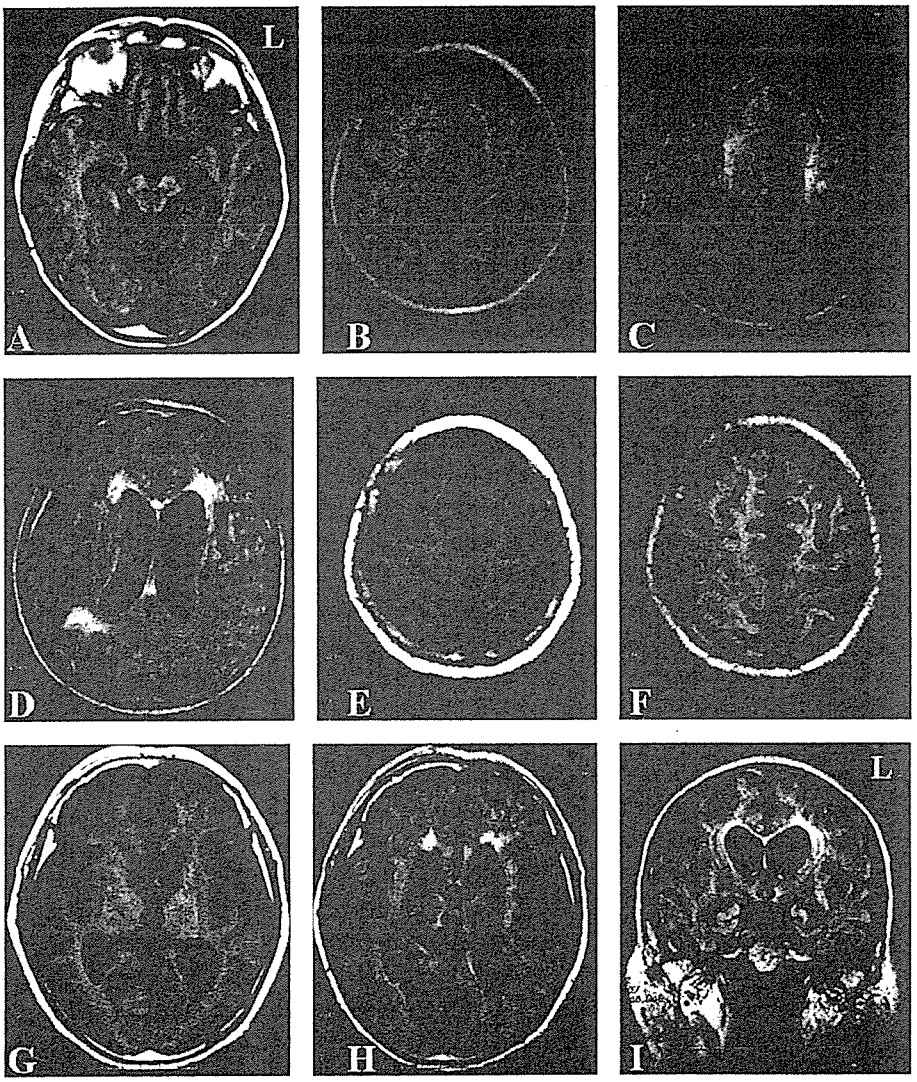

Fig. 1 Magnetic resonance images taken at age 63 (A–D) and age 66 (E–I) show supratentorial ventricular dilation and prominent cortical sulci due to moderate to severe cortical atrophy. There is mild to moderate non-specific cerebral cortical atrophy without significant laterality. The hippocampal formation as well as basal ganglia, appears to be normal in size (A–C). Periventricular hyperintensity of a moderate degree suggests that diffuse ischemia was present (D). There is progressive mild atrophy in the paracentral cortex with predominance on the left side (B, C, E, F). The bilateral putamina are atrophic without signal decrease indicative of increased iron deposition (G, H). The hippocampal formation associated with dilatation of the inferior horn of the lateral ventricles is also noted (I). There are the hypointense lesions at the level of the globus pallidus and hyperintense lesions in the cerebral white matter (I). (A, B, E, G): T1WI (TR 440, TE 16); (C, D, F, H, I): fluid attenuated inversion recovery (FLAIR) (TR 8802, TE 112).

tered for his extrapyramidal symptoms. At age 64, he had an episode of pneumonia. Subsequently, he developed dysphagia and because of subsequent walking disturbance he was limited to wheelchair conveyance. When he suffered from aspiration pneumonia at age 65, tracheotomy and percutaneous endoscopic gastrostomy (PEG) were carried out. He did not show any spontaneous speech. HMPAO-SPECT revealed diffuse cerebral hypoperfusion that was particularly prominent in the left frontal lobe. MRI showed severe cortical atrophy and enlargement of the lateral ventricles as well as dilatation of the central sulci and thinning of the corpus callosum. The left paracentral gyrus was significantly atrophic. The hippocampal formation also showed atrophy of a moderate degree. The bilateral putamen was atrophic but with no signal alteration suggestive of increased iron deposition. Using fluid attenuated inversion recovery (FLAIR) images, there were hyperintense lesions in the cerebral white matter and hypointense lesions in the globus pallidus (Fig. 1E–I). He died of aspiration pneumonia at age 67 and was tentatively diagnosed as having an atypical dementia. The patient's past medical history was acute hepatitis at age 30. Family history revealed that the patient's father died of cerebral infarction at age 92. However, no neurodegenerative diseases were recorded in the patient's family.

Macroscopic neuropathology

The harvested and fixed brain weighed 950 and 810 g, respectively. A severe atrophy and an enlargement of the sulci were present at the frontal lobes (Fig. 2A,B). The atrophy of the operculum and enlargement of the central sulcus were prominent in the left hemisphere. The cerebral arteries showed moderate atherosclerotic changes. Coronal slices disclosed that cortical gray matter was much thinner than normal in the frontal cortex and the lateral ventricles were enlarged. The anterior portion of the corpus callosum was atrophic. The head of the caudate nucleus

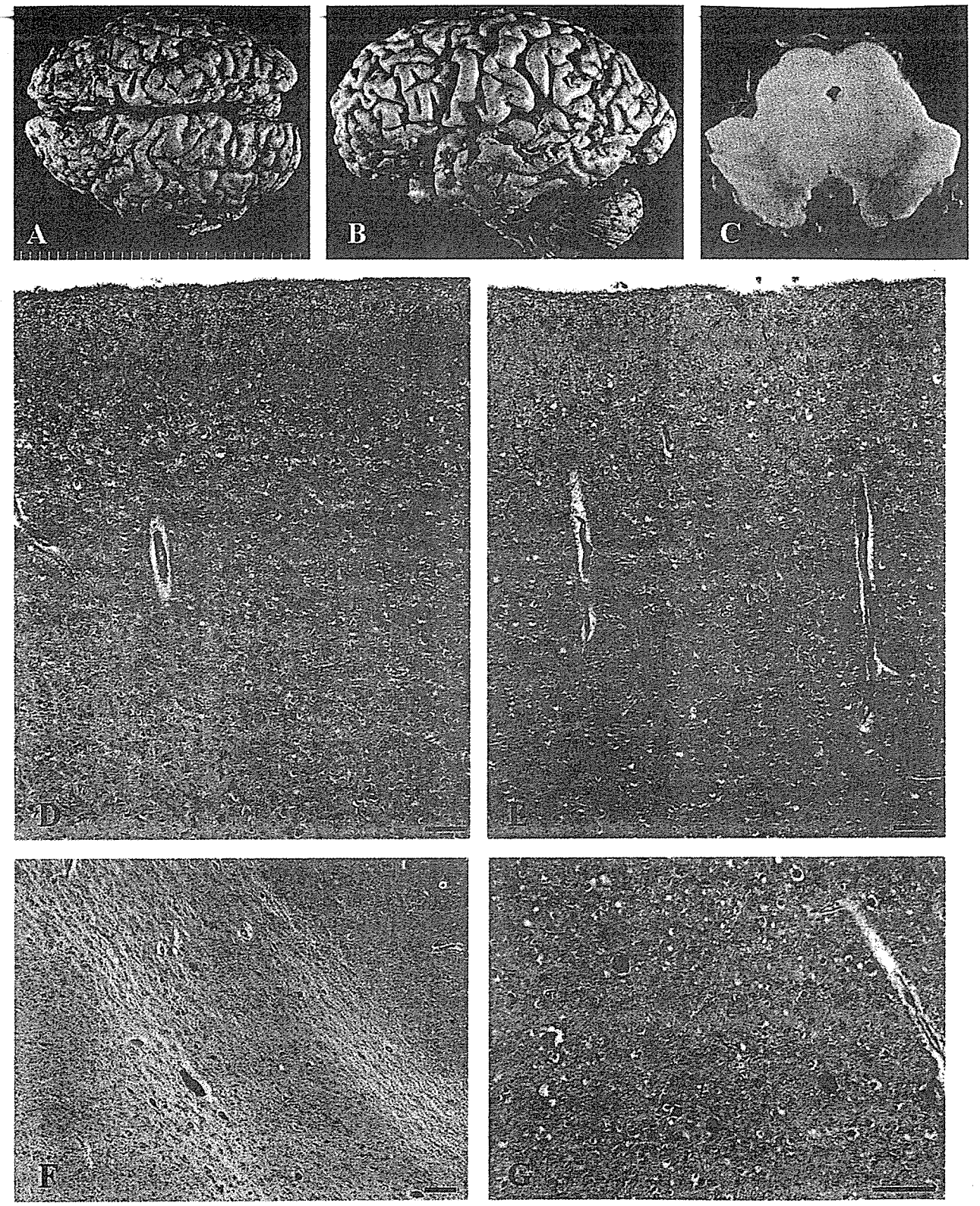

Fig. 2 (A, B, C). Macroscopic appearance of the proband's brain. Severe atrophy is present in the bilateral frontal lobes (A, B). Note the severe atrophy of the left operculum. Axial section of the midbrain shows severe depigmentation of the substantia nigra (C). Sections of the superior frontal cortex (D), temporal cortex (E), substantia nigra (F) and precentral gyrus (G). Severe neuronal loss and gliosis are present in the cerebral cortex. Note the neuronal loss and gliosis are more severe in the superior frontal cortex. Severe neuronal loss and extraneuronal pigment are present in the substantia nigra (F). Numerous ballooned neurons are seen in the precentral cortex (G). (D–G), Haematoxylin-eosin. Scale bars: (D–G), 100 μm.

and globus pallidus were moderately atrophic. Although the substantia nigra showed reduced pigmentation (Fig. 2C), the color of the locus coeruleus was slightly reduced. Frozen tissue was not obtained at the time of autopsy.

Microscopic neuropathology

The neocortex showed severe neuronal cell loss and gliosis, with moderate to severe spongy state in the upper layers of the frontal and cingulate cortices (Fig. 2D,E). The frontal operculum was also severely affected. In the cerebral cortex, ischemic neurons were occasionally observed. In the fifth layer of the precentral cortex, the gliosis was more severe than in the other cortical layers. Severe neuronal loss and gliosis were seen in the globus pallidus interna (Fig. 3A). Mild to moderate neuronal loss and gliosis were present in the claustrum, the head of caudate nucleus, putamen, globus pallidus externa, thalamus and the amygdala. Ballooned neurons were numerous in the frontal and cingulate cortex, and occasionally seen in the temporal, parietal cortex as well as in the claustrum (Fig. 2G). They were immunolabeled using antibody raised against neurofilament. In the hippocampus and parahippocampus, mild neuronal loss and gliosis as well as a few neurofibrillary tangles were present.

In the cerebellum, the dentate nucleus showed moderate neuronal loss and gliosis that were more severe in the right side. Grumose degeneration was also present in the neurons of the dentate nucleus. Although ischemic neurons were occasionally present in the Purkinje cell layer, the number of neurons in the cerebellar cortex was relatively well populated. Severe neuronal loss and extra neuronal melanin deposits were observed in the substantia nigra (Fig. 2F). Neuronal loss and gliosis were also present in the locus coeruleus. Neurofibrillary tangles were present in the periaqueductal gray matter, occulomotor nerve nucleus, substantia nigra, locus coeruleus and raphe nucleus. The spheroids were occasionally observable present in the substantia nigra. Frontopontine and pyramidal tracts showed mild loss of myelinated fibers suggesting mild degenerative condition.

Using modified Gallyas-Braak method, various argentophilic deposits were seen in the neurons and glial cells (Fig. 3B–N). In the cerebral cortex, numerous Gallyas-Braak positive neurons were seen in the frontal, insular, parietal and temporal cortex in which neuronal loss and gliosis were severe. Astrocytic plaques were also numerous in the frontal, temporal and parietal cortex. In addition, Gallyas-Braak positive neurons and astrocytic plaques were also observed in the occipital cortex. The argentophilic threads were abundant in the frontal, temporal, parietal cortex as well as in the basal ganglia and brainstem nuclei. Numerous argentophilic threads were also seen in the white matter of the cerebrum, cerebellum and brainstem. Frequency of Gallyas-Braak positive deposits and degree of neuronal loss and gliosis are summarized in the Table 1. There were no senile plaques, no Pick bodies or Lewy bodies in the cerebrum, cerebellum and brainstem. In the right parietal lobe, there was an organizing infarct that was identified as ischemic white matter lesion using MRI (Fig. 1).

DISCUSSION

We describe a case of CBD with non-fluent aphasia as an initial manifestation followed by dementia, parkinsonism and pyramidal signs. Although clinical appearance of the patient was unusual when compared with typical CBD, neuropathologic findings were consistent with the recent neuropathologic criteria of CBD.[24] Unfortunately, molecular analysis was impossible because the frozen tissue was not available at the time of autopsy. However, we believe that the present case is sporadic because of no apparent family history of neurodegenerative diseases.

Corticobasal degeneration is a relatively rare disorder and is clinically characterized by an akineto-rigid syndrome unresponsive to L-DOPA with dystonic postures, apraxia and a marked asymmetry of symptoms.[4,6,24] According to the analysis of 14 pathologically confirmed CBD cases, limb clumsiness and tremor were common symptoms followed by rigidity, apraxia, dystonia and dementia.[7] Cognitive dysfunction of CBD has been considered as rare or late manifestations.[4,7,25,26] In fact, one study showed that prominent sensory symptoms, isolated speech disturbance and behavioral disturbance were rare initial presentations of CBD.[26] The diagnostic research criteria of CBD in 1994 mentioned that early dementia was an exclusion criteria for the diagnosis of CBD.[27]

As the number of autopsy-confirmed CBD increased, cognitive impairment is now widely accepted as a common clinical feature.[4,6,12,13,24] In fact, the present case showed difficulty in simple arithmetic calculations and dementia in the clinical course. Particularly interesting is the fact that several types of aphasia have been reported in association with CBD.[4] However, only limited cases of pathologically confirmed CBD showed progressive aphasia as an initial presentation (Table 2).[13–21] According to these reports, clinical heterogeneity of progressive aphasia was present in the individuals with CBD. Although the severe atrophy of the operculum of the left inferior frontal gyrus, we cannot clearly show the specific regions in association with progressive aphasia in the present case. Because the present individual had seven years clinical course, it was difficult to analyze clinicopathological correlation between the final pathologic changes and initial clinical symptoms.

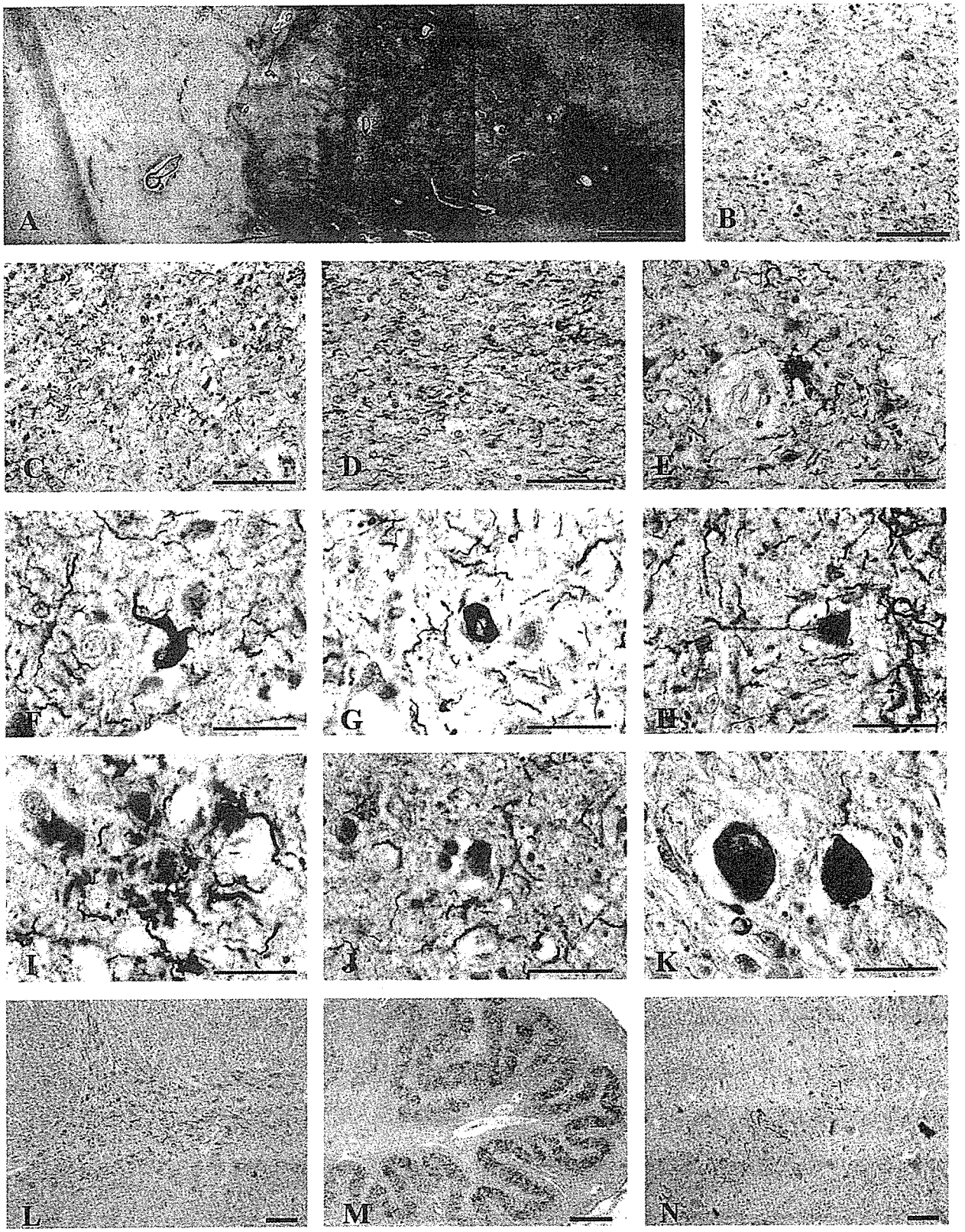

Fig. 3 (A). Macroscopic appearance of the basal ganglia. Severe gliosis is present in the globus pallidus. Note the gliosis is more prominent in the globus pallidus interna. Sections of the globus pallidus (B), superior frontal gyrus (C–J), substantia nigra (K), basis pontis (L), inferior olivary nucleus (M) and dentate nucleus of the cerebellum (N). Various argentophilic deposits (neurofibrillary tangles, argyrophilic threads, astrocytic plaques) are seen in the neurons and glial cells. (A), Holzer stain; (B–N), modified Gallyas-Braak stain. Scale bars: (A) 2 mm (B, L, N) 100 μm (C–K) 50 μm (M) 0.5 mm.

Table 1 Frequency of Gallyas-Braak positive deposits and degree of neuronal loss and gliosis

	GBP	AP	AT	Neuronal loss/Gliosis
Cerebrum				
Frontal cortex	3	3	severe	severe/severe
Cingulate cortex	3	3	severe	severe/severe
Temporal cortex	2	3	severe	severe/severe
Insular cortex	3	3	severe	severe/severe
Parietal cortex	2	3	severe	severe/severe
Motor cortex	3	3	severe	moderate/severe
Sensory cortex	2	2	severe	moderate/moderate
Occipital cortex	1	1	mild	mild/mild
Amygdala	3	3	severe	mild/moderate
Hippocampus	3	1	severe	mild/moderate
Dentate gyrus	1	0	moderate	mild/mild
Subiculum	3	1	moderate	mild/moderate
Entorhinal cortex	3	2	severe	mild/moderate
Caudate nucleus	2	0	severe	moderate/moderate
Putamen	2	0	severe	moderate/moderate
Claustrum	2	1	severe	mild/mild
Globus pallidus interna	2	1	severe	severe/severe
Globus pallidus externa	2	0	moderate	severe/severe
Thalamus	1	0	mild	moderate/moderate
Hypothalamus	2	1	moderate	mild/mild
Substantia innominata	2	0	moderate	mild/mild
Cerebellum				
Cortex	0	0	moderate	mild/mild
Dentate nucleus	1	0	moderate	moderate/moderate
Midbrain				
Periaqueductal gray	2	2	severe	moderate/moderate
Oculomotor nerve nuclei	3	0	severe	none/mild
Red nucleus	1	2	severe	mild/mild
Substantia nigra	3	0	severe	severe/severe
Pons				
Locus coeruleus	3	0	severe	mild/mild
Raphe nucleus	3	0	severe	mild/mild
Basis pontis	1	1	severe	mild/mild
Medulla				
Hypoglossal nerve nucleus	0	0	moderate	mild/mild
Dorsal motor nucleus of vagus	1	0	moderate	mild/mild
Lateral reticular nucleus	3	0	moderate	mild/mild
Inferior olivary nucleus	1	0	severe	none/moderate
Accessory olivary nucleus	1	0	moderate	mild/mild

AP, Astrocytic plaques; AT, Argentophilic threads; GBN, Gallyas-Braak positive neurons. Semi quantitative scale 0 = no GBN/AP, 1 = up to 5 GBN/AP/10× objective, 2 = 5–10 GBN/AP/10 × objective, 3 = 10> GBN/Aps.

Table 2 The previous reported cases of pathologically confirmed corticobasal degeneration associated with progressive aphasia

Author reference (No) (year)	Age at onset	Age at death	Handedness	Type of PA	Other initial symptoms	Most affected cerebral area
Lippa *et al.*[17] (1990)	72	78	Right	Non-fluent	None	Left-parasylvian
Lippa *et al.*[16] (1991)	66	68	NA	Transcortical expressive		Left-SFG
Lang AE[21] (1992)	64	73	NA	NA	none	NA
Arima *et al.*[14] (1994)	64	73	Right	Amnestic	Dysarthria hearing loss	Left-STG frontal operculum
Sakurai *et al.*[19] (1996)	64	72	Right	Amnestic	Hearing loss	Right-frontal
Ikeda *et al.*[15] (1996)	58	67	Right	Sensory	hearing loss	Left-STG
Mimura *et al.*[18] (2001)	62	65	Right	Transcortical motor	None	Left-IFG frontal operculum
Ferrer *et al.*[20] (2003)	66	73	Right	NA	none	NA
Present case	60	67	Right	Non-fluent	Difficulty in calculation	Left-IFG frontal opperculum

IFG, inferior frontal gyrus; NA, not available; PA, progressive aphasia; SFG, superior frontal gyrus; STG, superior temporal gyrus. The individuals of Arima *et al.*[14] and Sakurai *et al.*[19] might be identical.

Functional neuroradiological images may help to identify the responsible anatomic area of progressive aphasia of CBD.

Any neuropathologic basis of primary progressive aphasia remains uncertain. According to the many autopsy analyzes of primary progressive aphasia, approximately 60% of patients showed non-specific focal (or lobar) atrophy or dementia lacking distinctive histology, while 20% of patients showed Alzheimer's disease.[13] In the remaining 20% with primary progressive aphasia, Pick's disease and ubiquitin immunopositive inclusion disease were reported.[13] Therefore, only a limited number of cases were pathologically confirmed CBD with progressive aphasia. In the present case, the clinical presentation was unusual as a typical primary progressive aphasia by Mesulam in a rigorous manner.[13] However, we believe that the present case will provide important information to understand clinical heterogeneity of CBD.

Pyramidal signs and symptoms of CBD are relatively common features.[3,7,8,26,28] However, they have not been well analyzed because extrapyramidal signs are usually emphasized in the individuals with CBD.[3] The patient here described showed hyperreflexia in the extremities and pathologic reflexes in the latter half of the clinical course. Neuropathologically, there were the severe gliosis in the fifth layer of the motor cortex as well as pyramidal tract degeneration at the basis pontis and pyramids of the medulla obloganta. This finding strongly supports the recent findings of clinicopathologic correlation of pyramidal symptoms in CBD.[1,2,24,25]

The cortical atrophy, ballooned neurons and degeneration of the substantia nigra have been emphasized as the neuropathologic features of CBD.[24] Recent neuropathologic criteria emphasize Gallyas-Braak positive or tau-immunoreactive lesions in neurons, glia and cell processes such as astrocytic plaques and thread-like lesions in both white matter and gray matter.[29] In the present case, astrocytic plaques were numerous and present along with neuronal loss in focal cortical regions. In addition, they were also seen in the occipital cortex. The severity and distribution of abnormal Gallyas-Braak positive structures may be considerably different in each case of CBD. Systematic neuropathologic analysis of abnormal tau deposits is important in order to explain the clinical heterogeneity of CBD.

Information of MRI findings of CBD was limited. According to the recent literature, the most common findings are prominent cortical atrophy in the paracentral parietal region and the superior frontal gyrus, corpus callosum atrophy as well as the subcortical and periventricular white matter signal changes of MRI.[30,31] In the present case, the cortical atrophy was relatively diffuse and hippocampal formation was also atrophic. At the end of the clinical course, the proband's MRI showed hypointensity in the globus pallidus and hyperintense ones in the cerebral white matter using FLAIR images. In addition, progressive atrophy was observed in the bilateral putamen. The previous report showed that the hyperintense lesions of cerebral white matter might reflect demyelination.[32] In our case, there were severe degenerative conditions with argentophilic deposits and gliosis in the cerebral white matter. We need to be careful in interpretation of the hyperintense lesions of T2 weighted and FLAIR images in the subcortical area. In some instances, those hyperintense lesions are present in healthy individuals as ischemic lesions.[33]

In addition to the bilateral atrophy of the putamen,[34] the present case showed a T2-weighted signal hypointense legion in the globus pallidus in CBD. In a pathologic examination, the proband's brain showed severe degeneration of the globus pallidus. However, the interpretation of the MRI signal change of globus pallidus and atrophy of the putamen is difficult and must be cautious for the following reasons. First, the globus pallidus may show hypointensity using T2WI or FLAIR images even in the normal individuals because of iron accumulation. Second, it was difficult to analyze the exact size of the putamen in this case by autopsy material. Future analyzes using MRI may enable investigators to reach increasing accurate diagnosis of CBD.

We report an individual diagnosed with CBD who showed primary progressive aphasia. Neuropathologically, numerous argyrophilic structures, including astrocytic plaques, were observed in the neurons and glia. The pyramidal tract degeneration and loss of Bets cells were also present. This report will provide useful knowledge to understanding the clinical heterogeneity of CBD. The better clinical and radiological criteria may warrant the accurate diagnosis of CBD.

ACKNOWLEDGMENTS

This study was supported in part by Grants-in-Aid for Scientific Research (The Japan Society for the Promotion of Science 15600226). We gratefully acknowledge W. Robert and R. Umehara for editing the manuscript.

REFERENCES

1. Rebeiz JJ, Kolodny EH, Richardson EP Jr. Corticodentatonigral degeneration with neuronal achromasia: a progressive disorder of late adult life. *Trans Am Neurol Assoc* 1967; **92**: 23–26.
2. Rebeiz JJ, Kolodny EH, Richardson EP Jr. Corticodentatonigral degeneration with neuronal achromasia. *Arch Neurol* 1968; **18**: 20–33.

3. Tsuchiya K, Murayama S, Mitani K *et al.* Constant and severe involvement of Betz cells in corticobasal degeneration is not consistent with pyramidal signs: a clinicopathological study of ten autopsy cases. *Acta Neuropathol (Berl)* 2005; **109**: 353–366.
4. Graham NL, Bak TH, Hodges JR. Corticobasal degeneration as a cognitive disorder. *Mov Disord* 2003; **18**: 1224–1232.
5. Litvan I, Grimes DA, Lang AE *et al.* Clinical features differentiating patients with postmortem confirmed progressive supranuclear palsy and corticobasal degeneration. *J Neurol* 1999; **246** (Suppl. 2): II1–5.
6. Mahapatra RK, Edwards MJ, Schott JM, Bhatia KP. Corticobasal degeneration. *Lancet Neurol* 2004; **3**: 736–743.
7. Wenning GK, Litvan I, Jankovic J *et al.* Natural history and survival of 14 patients with corticobasal degeneration confirmed at postmortem examination. *J Neurol Neurosurg Psychiatry* 1998; **64**: 184–189.
8. Kompoliti K, Goetz CG, Boeve BF *et al.* Clinical presentation and pharmacological therapy in corticobasal degeneration. *Arch Neurol* 1998; **55**: 957–961.
9. Mesulam M, Weintraub S, Parrish T, Gitelman D. Primary progressive aphasia: reversed asymmetry of atrophy and right hemisphere language dominance. *Neurology* 2005; **64**: 556–557.
10. Mesulam MM. Slowly progressive aphasia without generalized dementia. *Ann Neurol* 1982; **11**: 592–598.
11. Mesulam MM. Primary progressive aphasia – differentiation from Alzheimer's disease. *Ann Neurol* 1987; **22**: 533–534.
12. Mesulam MM. Primary progressive aphasia. *Ann Neurol* 2001; **49**: 425–432.
13. Mesulam MM. Primary progressive aphasia – a language-based dementia. *N Engl J Med* 2003; **349**: 1535–1542.
14. Arima K, Uesugi H, Fujita I *et al.* Corticonigral degeneration with neuronal achromasia presenting with primary progressive aphasia: ultrastructural and immunocytochemical studies. *J Neurol Sci* 1994; **127**: 186–197.
15. Ikeda K, Akiyama H, Iritani S *et al.* Corticobasal degeneration with primary progressive aphasia and accentuated cortical lesion in superior temporal gyrus: case report and review. *Acta Neuropathol (Berl)* 1996; **92**: 534–539.
16. Lippa CF, Cohen R, Smith TW, Drachman DA. Primary progressive aphasia with focal neuronal achromasia. *Neurology* 1991; **41**: 882–886.
17. Lippa CF, Smith TW, Fontneau N. Corticonigral degeneration with neuronal achromasia. A clinicopathologic study of two cases. *J Neurol Sci* 1990; **98**: 301–310.
18. Mimura M, Oda T, Tsuchiya K *et al.* Corticobasal degeneration presenting with nonfluent primary progressive aphasia: a clinicopathological study. *J Neurol Sci* 2001; **183**: 19–26.
19. Sakurai Y, Hashida H, Uesugi H *et al.* A clinical profile of corticobasal degeneration presenting as primary progressive aphasia. *Eur Neurol* 1996; **36**: 134–137.
20. Ferrer I, Hernandez I, Boada M *et al.* Primary progressive aphasia as the initial manifestation of corticobasal degeneration and unusual tauopathies. *Acta Neuropathol (Berl)* 2003; **106**: 419–435.
21. Lang AE. Cortica basal degeneration presenting with progressive loss fo speech output and orofacial dyspraxis. *J Neurol Neurosurg Psychiatry* 1992; **55**: 1101.
22. Tsuchiya K, Ishizu H, Nakano I *et al.* Distribution of basal ganglia lesions in generalized variant of Pick's disease: a clinicopathological study of four autopsy cases. *Acta Neuropathol (Berl)* 2001; **102**: 441–448.
23. Takao M, Ghetti B, Yoshida H *et al.* Early-onset dementia with Lewy bodies. *Brain Pathol* 2004; **14**: 137–147.
24. Dickson DW, Bergeron C, Chin SS *et al.* Office of Rare Diseases neuropathologic criteria for corticobasal degeneration. *J Neuropathol Exp Neurol* 2002; **61**: 935–946.
25. Gibb WR, Luthert PJ, Marsden CD. Corticobasal degeneration. *Brain* 1989; **112**: 1171–1192.
26. Rinne JO, Lee MS, Thompson PD, Marsden CD. Corticobasal degeneration. A clinical study of 36 cases. *Brain* 1994; **117**: 1183–1196.
27. Lang AE, Riley DE, Bergerson C. *Cortical-Basal Ganglionic Degeneration.* Philadelphia: W.B. Saunders, 1994.
28. Boeve BF, Maraganore DM, Parisi JE *et al.* Pathologic heterogeneity in clinically diagnosed corticobasal degeneration. *Neurology* 1999; **53**: 795–800.
29. Valk J, Barkhof F, Scheltens P. Coricobasal degenration. In: Valk J, Barkhof F, Scheltens P (eds) *Magnetic Resonance in Dementia.* Heidelberg: Springer-Verlag, 2002.
30. Hauser RA, Murtaugh FR, Akhter K, Gold M, Olanow CW. Magnetic resonance imaging of corticobasal degeneration. *J Neuroimaging* 1996; **6**: 222–226.
31. Josephs KA, Tang-Wai DF, Edland SD *et al.* Correlation between antemortem magnetic resonance imaging findings and pathologically confirmed corticobasal degeneration. *Arch Neurol* 2004; **61**: 1881–1884.
32. Doi T, Iwasa K, Makifuchi T, Takamori M. White matter hyperintensities on MRI in a patient with cortico-

basal degeneration. *Acta Neurol Scand* 1999; **99**: 199–201.

33. Takao M, Koto A, Tanahashi N, Fukuuchi Y, Takagi M, Morinaga S. Pathologic findings of silent hyperintense white matter lesions on MRI. *J Neurol Sci* 1999; **167**: 127–131.
34. Tokumaru AM, O'Uchi T, Kuru Y, Maki T, Murayama S, Horichi Y. Corticobasal degeneration: MR with histopathologic comparison. *AJNR Am J Neuroradiol* 1996; **17**: 1849–1852.

Correlation of visual hallucinations with occipital rCBF changes by donepezil in DLB

Abstract—The authors explored the neural substrate of visual hallucinations in dementia with Lewy bodies (DLB) by investigating changes in regional cerebral blood flow (rCBF) and psychiatric symptoms, before and after cholinesterase inhibitor treatment. Twenty subjects with DLB were treated with donepezil for a 12-week period. Hallucinations attenuated while receiving therapy, whereas occipital rCBF focally increased, suggesting that functional visual association cortex deficits may cause visual hallucinations in patients with DLB.

NEUROLOGY 2006;66:935–937

T. Mori, MD; M. Ikeda, MD, PhD; R. Fukuhara, MD, PhD; P.J. Nestor, PhD, FRACP; and H. Tanabe, MD, PhD

Dementia with Lewy bodies (DLB) is characterized by recurrent visual hallucinations, fluctuating cognitive impairment, and parkinsonism.[1] There is consistent evidence that cholinesterase inhibitors are effective in DLB, with visual hallucinations being particularly responsive to treatment.[2]

In contrast to Alzheimer disease (AD), which shows bilateral parietotemporal dysfunction, DLB is associated with severe occipital hypometabolism and hypoperfusion on fluorodeoxyglucose positron emission tomography (FDG-PET)[3] and SPECT.[4] No previous studies have addressed the possible relationships between changes in regional cerebral blood flow (rCBF) and psychiatric symptoms in DLB during cholinesterase inhibitor treatment. We hypothesized that the observed improvement in visual hallucinations with cholinesterase inhibitor medication could be associated with changes in rCBF, thus offering an insight into the neural substrate of visual hallucinations in patients with DLB.

Methods. Participants were recruited from a university hospital outpatient clinic. Twenty patients (age 77.4 ± 5.3 years; 10 women) with probable DLB, according to consensus guidelines[1] who were living with a responsible caregiver were selected. Cases met consensus criteria, but, because of the nature of this study, a history of visual hallucinations was a mandatory inclusion criterion. Furthermore, 18 cases had reported visual hallucinations in the month before scanning. Exclusion criteria included 1) Hoehn and Yahr score >3, 2) MRI evidence of focal brain lesions, 3) neuroleptic or antiparkinsonian therapy. Written informed consent was obtained from all subjects or their relatives.

Patients were treated for 12 weeks with donepezil according to Japanese dosing guidelines for AD. Donepezil was commenced at 3 mg/day. After 2 weeks, patients were reassessed for adverse effects. Patients who were tolerating therapy then had their dose titrated up to 5 mg/day for the remaining 10 weeks.

The Neuropsychiatric Inventory (NPI)[5] and the Mini-Mental State Examination (MMSE) were administered at baseline and 12 weeks. The NPI is a validated, caregiver-based instrument for measuring behavioral changes in dementia, such as delusions and hallucinations. The two-tailed Wilcoxon signed-rank test for paired samples was used for statistical analysis of the total NPI and MMSE scores, and the cutoff for significance between baseline and 12-week assessments was set at $p < 0.05$. We also made use of the two-tailed Wilcoxon signed-rank test to examine changes in the NPI subscales: the significance was set at $p < 0.05$ after Bonferroni correction (nominal α of 0.05/10 = 0.005). All SPECT scans were carried out under identical conditions using 740 MBq technetium-99m hexamethyl-propyleneamine oxine (^{99m}Tc-HMPAO) with patients' eyes closed (monitored through the procedure by a radiologist) in a quiet, dimly lit room. The SPECT system used a four-head rotating gamma camera equipped with high-resolution low-energy collimators, providing an in-plane spatial resolution of 7.5 mm full width at half maximum (FWHM). Data were obtained from the 140-keV photo peak (10% window) over a 360-degree rotation and 128 × 128 matrix. The slice thickness and axial resolution of SPECT images were 2.0 mm. The step-and-shoot format was used (acquisition time: 20 s/step; zoom factor: 1.33). Transaxial images of ^{99m}Tc-HMPAO SPECT were reconstructed by filtered back projection using Butterworth and Ramp filters (cutoff frequency 0.12 cycle/cm) with attenuation correction (Chang, 0.08/cm).

Data were analyzed using MATLAB 6.5 (The MathWorks. Inc.) and SPM99 (Wellcome Department of Cognitive Neurology, London, UK).[6] Raw images were spatially transformed to the SPM99 SPECT template. The spatially normalized images were resliced to a 2 × 2 × 2-mm voxel size and then smoothed with an isotropic 16-mm FWHM Gaussian filter.

The SPM analysis used the one scan per subject, paired t test model between scans at baseline and 12 weeks. Each individual image was normalized by proportional scaling across the entire data set to a mean of 50 mL/100 mL/min. The threshold images show voxels, which are different using $p < 0.001$ (uncorrected).

Results. The mean scores (± SD) at baseline for the MMSE and total NPI were 17.2 ± 5.8 and 30.0 ± 20.0 (table 1). At 12 weeks, there was improvement in both MMSE (20.5 ± 5.8; $z = -2.613$, $p = 0.009$) and total NPI score (8.2 ± 7.6; $z = -3.465$, $p = 0.0006$). Among the NPI subscales, the most improvement was in hallucinations ($z = -3.724$, $p = 0.0002$). All hallucinations were visual in type.

The figure and table 2 show the voxels of increased rCBF compared with baseline ($p < 0.001$ uncorrected). All significant changes were restricted to the occipital lobes. The statistical peaks in the right occipital region (p corrected = 0.144, $k = 741$, $t = 5.55$, $Z = 4.23$, peak coordinates $x = 38$, $y = -84$, $z = -8$) and the left occipital region

From the Department of Neuropsychiatry (T.M., M.I., R.F., H.T.), Ehime University School of Medicine, Ehime, Japan; and University of Cambridge, Neurology Unit, Addenbrooke's Hospital (P.J.N.), Cambridge, United Kingdom.

Supported by the Higher Brain Function Groups of the Department of Neuropsychiatry, Ehime University School of Medicine.

Disclosure: The authors report no conflicts of interest.

Received May 16, 2005. Accepted in final form December 8, 2005.

Address correspondence and reprint requests to Dr. Manabu Ikeda, Department of Neuropsychiatry, Ehime University School of Medicine, Toon city, Ehime 791-0295, Japan; e-mail: mikeda@m.ehime-u.ac.jp

Table 1 *Changes in the scores of MMSE, total scores of NPI and NPI subscales for patients with DLB using cholinesterase inhibitor medication (N = 20)*

	Baseline		12 Wk			
	Mean	SD	Mean	SD	z*	p
MMSE	17.2	5.8	20.5	5.8	−2.613	0.0090†
NPI total score	30.0	20.0	8.2	7.6	−3.465	0.0006‡
Delusions	6.0	4.5	2.3	2.7	−2.755	0.0058
Hallucinations	6.4	4.0	1.4	1.8	−3.724	0.0002§
Agitation/aggression	2.9	4.5	0.8	1.8	−1.956	0.0505
Depression/dysphoria	1.7	2.4	0.8	2.0	−1.423	0.1549
Anxiety	2.8	4.0	0.6	1.7	−1.988	0.0461
Euphoria/elation	0.0	0.0	0.0	0.0		
Apathy/indifference	3.1	3.6	0.8	1.7	−2.267	0.0229
Disinhibition	0.8	2.3	0.2	0.9	−1.069	0.2850
Irritability/lability	1.8	3.1	0.9	1.9	−1.125	0.2604
Aberrant motor behavior	2.0	3.3	1.0	2.8	−0.980	0.3270

* Wilcoxon signed-rank tests.
† Greater change at 12 weeks than that at baseline ($z = -2.613$, $p = 0.0090$).
‡ Less change at 12 weeks than that at baseline ($z = -3.465$, $p = 0.0006$).
§ Less change at 12 weeks than that at baseline ($z = -3.724$, $p = 0.0002$).

MMSE = Mini-Mental State examination; NPI = Neuropsychiatric Inventory; DLB = dementia with Lewy bodies.

(p corrected = 0.220, k = 825, t = 5.28, Z = 4.09, peak coordinates $x = -36$, $y = -84$, $z = -8$) corresponded to visual association cortices.

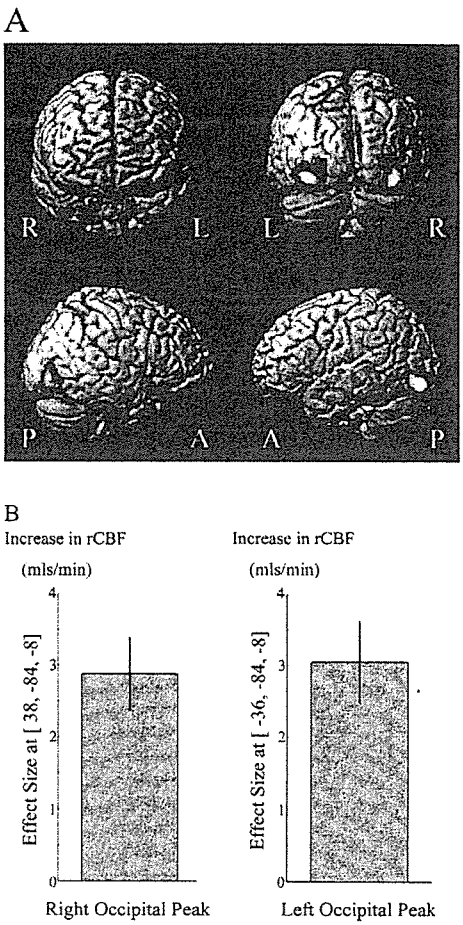

Figure. (A) Significant perfusion increases in regional cerebral blood flow in patients with dementia with Lewy bodies at 12 weeks compared with at baseline using cholinesterase inhibitor medication (N = 20) (statistical parametric mapping analysis [paired t test, $p < 0.001$ uncorrected]). (B) The magnitude of the effect at baseline and with donepezil for the right and left occipital peaks.

Discussion. We demonstrated that cognitive function and psychiatric symptoms, particularly visual hallucinations, improved and that occipital rCBF increased with donepezil therapy in DLB. Previous SPECT and FDG-PET studies in patients with DLB reported dysfunction in the occipital area compared with AD patients and controls.[3,4] Some reports have suggested that visual hallucinations are specifically associated with occipital dysfunction[7]; furthermore, occipital cholinergic deficits have been reported in the brains of patients with DLB.[8] The current results suggest that occipital cholinergic deficits, occipital hypoperfusion, and visual hallucinations may be directly interrelated.

While clinicopathologic studies in DLB have demonstrated extensive neocortical cholinergic deficits that correlate with clinical symptoms,[9] cortical Lewy bodies are found in the anterior frontal, temporal, insular, and cingulate cortices, but rarely in occipital cortex. Furthermore, reports have also suggested that there are no structural changes in gray matter on MRI in the occipital lobe of patients with DLB.[10] Functional imaging changes caused by DLB in the occipital area may not therefore be the result of underlying structural changes in the gray matter but instead may be caused by a lack of acetylcholine from presynaptic neurons originating in the forebrain or brainstem. In other words, we speculate that a significant component of the occipital perfusion defect previously described in DLB is physiologic. Patients with the posterior cortical atrophy variant of AD also have marked occipital cortex deficits seen on SPECT or PET but rarely hallucinate and have pathologic evidence of local neurodegeneration. Taken together, we propose that a specific lack of cholinergic inputs from the forebrain or brainstem, rather than a local destructive process, may therefore be a key to the genesis of visual hallucinations in DLB. This imbalance can be restored with cholinesterase inhibitors, suggesting that postsynaptic muscarinic receptors are relatively preserved, leading to an increase in occipital neuronal activity as indicated by improvement in cerebral perfusion.

Cholinergic transmission is also implicated in maintaining alertness, and it has been reported that

Table 2 Significant increase in regional cerebral blood flow in patients with dementia with Lewy bodies at 12 weeks compared with at baseline using cholinesterase inhibitor medication (N = 20)

					Peak coordinates*			
p Corrected	*k*	*t*	*Z* Score	*p* Uncorrected	*x*	*y*	*z*	Anatomic region
0.144	741	5.55	4.23	<0.000	38	−84	−8	Right inferior occipital lobe
0.220	825	5.28	4.09	<0.000	−36	−84	−8	Left inferior occipital lobe

* Coordinates in Talairach space and statistical parametric mapping analysis (paired t test, $p < 0.001$ uncorrected).

an increased level of alertness would be expected in order to reduce patients' tendencies to hallucinate. We cannot exclude a possible relationship between alertness and hallucinations in DLB. However, if improving visual hallucinations is purely a function of alertness, the association between a focal rCBF increase in occipital areas and improving visual hallucinations is difficult to reconcile. Therefore, it seems appropriate to speculate that the bilateral increase in occipital rCBF is specifically associated with improvement of visual hallucinations.

There are a few limitations in the present study. The first is sample size. It is difficult to recruit suitable patients with DLB for two SPECT scans in 12 weeks; however, it should be noted that this DLB cohort is larger than most previously studied by SPECT. Second, the absence of controls raises the possibility that occipital SPECT changes were nonspecific; nevertheless, the focal nature of the rCBF increase, in a highly plausible locus for visual hallucination, makes this interpretation seem less likely. Finally, we could not confirm the presence of visual hallucinations or control for the effects of fluctuating cognitive impairment during SPECT acquisition, but neither could most previous studies. Future studies assessing cognitive status and probing for the presence of hallucination immediately after image acquisition may offer further insights.

Acknowledgment

The authors thank Dr. Y. Sugawara and Prof. T. Mochizuki in the Department of Radiology, Ehime University School of Medicine, for advice and encouragement.

References

1. McKeith IG, Galasko D, Kosaka K, et al. Consensus guidelines for the clinical and pathologic diagnosis of dementia with Lewy bodies (DLB): report of the consortium on DLB international workshop. Neurology 1996;47:1113–1124.
2. McKeith I, Del Ser T, Spano P, et al. Efficacy of rivastigmine in dementia with Lewy bodies: a randomised, double-blind, placebo-controlled international study. Lancet 2000;356:2031–2036.
3. Ishii K, Imamura T, Sasaki M, et al. Regional cerebral glucose metabolism in dementia with Lewy bodies and Alzheimer's disease. Neurology 1998;51:125–130.
4. Lobotesis K, Fenwick JD, Phipps A, et al. Occipital hypoperfusion on SPECT in dementia with Lewy bodies but not AD. Neurology 2001;56:643–649.
5. Cummings JL, Mega M, Gray K, Rosenberg-Thompson S, Carusi DA, Gornbein J. The Neuropsychiatric Inventory: comprehensive assessment of psychopathology in dementia. Neurology 1994;44:2308–2314.
6. Ashburner J, Friston KJ. Nonlinear spatial normalization using basis functions. Hum Brain Mapp 1999;7:254–266.
7. Imamura T, Ishii K, Hirono N, et al. Visual hallucinations and regional cerebral metabolism in dementia with Lewy bodies (DLB). Neuroreport 1999;10:1903–1907.
8. Perry EK, Irving D, Kerwin JM, et al. Cholinergic transmitter and neurotrophic activities in Lewy body dementia: similarity to Parkinson's and distinction from Alzheimer disease. Alzheimer Dis Assoc Disord 1993;7:69–79.
9. Perry EK, Haroutunian V, Davis KL, et al. Neocortical cholinergic activities differentiate Lewy body dementia from classical Alzheimer's disease. Neuroreport 1994;5:747–749.
10. Middelkoop HA, van der Flier WM, Burton EJ, et al. Dementia with Lewy bodies and AD are not associated with occipital lobe atrophy on MRI. Neurology 2001;57:2117–2120.

21

Fronto-temporal dementia

M. Ikeda

INTRODUCTION

As dementia progresses, recognition skills become impaired in combination with delusions, agitation, feelings of worry, and depression, leading to a wide range of neuropsychiatric manifestations and disturbed behaviour (now frequently called behavioural and psychological symptoms of dementia [BPSD]) [1]. In recent years, there has been considerable progress in expanding the differential diagnosis of Alzheimer's disease (AD) with clinical characterisation of fronto-temporal dementia (FTD), dementia with Lewy bodies (DLB) and so on. These developments emphasise the need for disease specific management. Each dementia has its own characteristic behavioural profile. For example, patients with AD have higher rates of delusions than FTD patients. In DLB, visual hallucinations are prominent, whereas in FTD inappropriate eating behaviour and aggression are more pronounced. These BPSD are highly prevalent in patients with dementia and are a major source of difficulty and distress for caregivers. BPSD are one of the main reasons for hospital or nursing home placement of patients, and thus contribute greatly to the cost of caring for dementia patients. While a number of intervention studies have aimed to reduce the burden of caring for patients with dementia through family support and counselling of caregivers, few studies have focused on using pharmacotherapy or non-pharmacologic management to alleviate specific BPSD and reduce the care burden [2]. Although the aetiology of these neurodegenerative diseases is still unknown, treatment should be directed toward disease specific symptomatic improvement.

FTD is now included more in the comprehensive construct, fronto-temporal lobar degeneration (FTLD) [3], that comprises frontal type dementia, with other subtypes such as semantic dementia (SD) and progressive non-fluent aphasia (PA). In spite of the possibility that FTLD has been under-recognised clinically, it is thought to account for up to 20% of presenile dementia. The Cambridge group recently examined the prevalence of early-onset dementia in community-based study [4]. Of 108 cases identified, FTLD accounted for 17 patients (15.7%) and AD for 25%. The FTLD group included 13 FTD and two each with SD and PA. Almost one-third of cases with FTLD (29%) had a positive family history. In our consecutive series of 330 outpatients with dementia (hospital setting without age limitation), 42 (12.7%) had FTLD and 215 (65.1%) had AD; the FTLD group comprised 22 FTD, 15 SD and 5 PA [5]. In summary, these epidemiological studies, both in community-based and hospital-based samples, demonstrate that FTD is a more common cause of early-onset dementia than was previously recognised.

Manabu Ikeda, ■■■

Table 21.1 Behavioural features of FTD

Loss of social awareness and insight
Personal neglect
Disinhibition, impulsivity, restlessness (Going my way behaviour)
Distractibility and impersistence
Inertia, aspontaneity, loss of volition
Mental rigidity and inflexibility
Sterotypies, compulsivity
Stimulus-bound behaviour
Hyperorality and dietary changes

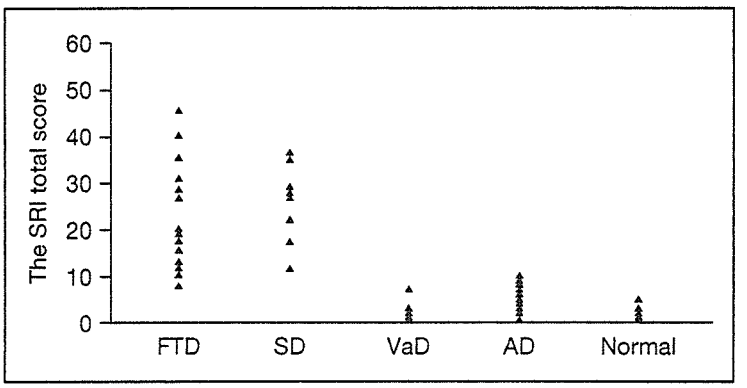

Figure 21.1 The SRI total score of FTD, SD, VaD, AD and normal control subjects (revised from reference [5]). The SRI provides scores for 5 domains' subscales (eating and cooking behaviours, roaming, speaking, movements, and daily rhythm). Each is scored for frequency and severity, and the total subscale score can be calculated by multiplying these two factors. The SRI total score is the sum of the 5 total subscore. Total score on the SRI of FTD and SD patient groups were higher than that of VaD patients, AD patients, and normal controls with very little overlap ($P < 0.0001$) [8].

Distinctive unusual behaviours of FTD, such as disinhibition, loss of social awareness, overeating, perseverative and stereotyped behaviour, and impulsivity, are serious obstacles to managing and caring for patients with FTD [6]. The main behavioural features of FTD are listed in Table 21.1. Patients with subtypes of FTLD, especially FTD and SD, exhibit very similar profiles of abnormal behaviour. Among these peculiar behavioural disturbances, stereotypic and eating behaviours are significantly more frequent in FTLD than in other types of dementia [7–9]. These behaviours are so characteristic of FTLD that they are important symptoms for discriminating between FTLD and AD (Figures 21.1 and 21.2).

There is no known treatment to delay the progression of FTD although non-pharmacological and pharmacological interventions may potentially help considerably with behavioural management [10, 11]. Thus far there have been no systematic efforts to manage or treat patients with FTD [12].

PRINCIPLES OF TREATMENT AND MANAGEMENT FOR CHALLENGING BEHAVIOURS

INSTRUCTION FOR CAREGIVERS

Education programs should be offered to families and caregivers to improve caregiver satisfaction and reduce the caregiver's burden. Lack of knowledge can contribute to caregiver